



# Andrographolide sulfonate downregulation of TLR3-TRIF and amelioration of airway inflammation caused by respiratory syncytial virus infection

Na Zhou<sup>1,2</sup>, Siyi Che<sup>2</sup>, Jiao Liu<sup>2</sup>, Zhenghong Jiang<sup>2</sup>, Luo Ren<sup>2,3</sup>, Yin Liu<sup>4</sup>, Enmei Liu<sup>2,3</sup>, Jun Xie<sup>2,3</sup>

<sup>1</sup>Department of Pediatrics, Bishan Hospital of Chongqing Medical University, Bishan County, Chongqing, China; <sup>2</sup>Pediatric Research Institute, Children's Hospital of Chongqing Medical University, Chongqing Key Laboratory of Child Rare Diseases in Infection and Immunity, Chongqing, China; <sup>3</sup>Department of Respiratory Medicine, Children's Hospital of Chongqing Medical University, National Clinical Research Center for Child Health and Disorders, Ministry of Education Key Laboratory of Child Development and Disorders, Chongqing Key Laboratory of Pediatrics, Chongqing, China; <sup>4</sup>State Key Laboratory of Innovative Natural Medicine and TCM Injections, Jiangxi Qingfeng Pharmaceutical Co. Ltd., Ganzhou, China

**Contributions:** (I) Conception and design: J Xie, N Zhou; (II) Administrative support: L Ren; (III) Provision of study materials or patients: J Liu, Y Liu; (IV) Collection and assembly of data: Z Jiang; (V) Data analysis and interpretation: N Zhou, S Che; (VI) Manuscript writing: All authors; (VII) Final approval of manuscript: All authors.

**Correspondence to:** Jun Xie, MD. Pediatric Research Institute, Children's Hospital of Chongqing Medical University, Chongqing Key Laboratory of Child Rare Diseases in Infection and Immunity, Chongqing, China; Department of Respiratory Medicine, Children's Hospital of Chongqing Medical University, National Clinical Research Center for Child Health and Disorders, Ministry of Education Key Laboratory of Child Development and Disorders, Chongqing Key Laboratory of Pediatrics, 136 Zhongshan Second Road, Yuzhong District, Chongqing 400014, China. Email: cyxiejun@126.com.

**Background:** Andrographolide sulfonate (Andro-S), a traditional Chinese medicine, is commonly used to treat pediatric respiratory tract infections in China. However, its therapeutic effects in infections caused by respiratory syncytial virus (RSV) have not been reported. We thus aimed to investigate the therapeutic effects of Andro-S using a mouse model of RSV infection-induced airway inflammation.

**Methods:** Immunocompromised (cyclophosphamide-treated) BALB/c mice were intranasally infected with RSV and treated with intranasal or intraperitoneal Andro-S once daily for five consecutive days, starting on the day of infection. Histopathological changes in the lung were evaluated using hematoxylin and eosin staining. Total inflammatory cell counts and macrophage, lymphocyte, neutrophil, and eosinophil counts in the bronchoalveolar lavage fluid (BALF) were microscopically determined. Interferon- $\gamma$  (IFN- $\gamma$ ) levels in the BALF were detected using enzyme-linked immunosorbent assay (ELISA). The messenger RNA levels of RSV nucleoprotein (N) and Toll-like receptors (TLRs) 1–9 in lung tissues were determined with quantitative real-time polymerase chain reaction (qRT-PCR). The protein levels of RSV N, RSV fusion protein (F), TLR2, TLR3, and TIR domain-containing adapter-inducing interferon- $\beta$  (TRIF) were detected via Western blot analysis.

**Results:** RSV infection caused lung inflammation, manifesting as bronchiolitis, alveolitis, and perivascular inflammation; increased the number of inflammatory cells; and elevated IFN- $\gamma$  levels in the BALF. Lung inflammation was positively correlated with pulmonary RSV N levels in infected mice. Intranasal Andro-S significantly downregulated RSV N, RSV F, TLR3, and TRIF protein expression in the lung and ameliorated lung inflammation in infected animals. However, intraperitoneal Andro-S showed no effects on lung inflammation caused by RSV infection.

**Conclusions:** Intranasal Andro-S inhibits RSV replication and ameliorates RSV infection-induced lung inflammation by downregulating TLR3 and TRIF. Therefore, intranasal administration may be a suitable drug delivery method for treating RSV infection.

**Keywords:** Andrographolide sulfonate (Andro-S); respiratory syncytial virus (RSV); lung inflammation; TLR3; TIR domain-containing adapter-inducing interferon- $\beta$  (TRIF)

Submitted May 08, 2024. Accepted for publication Jun 14, 2024. Published online Jul 09, 2024.

doi: 10.21037/jtd-24-752

View this article at: <https://dx.doi.org/10.21037/jtd-24-752>

## Introduction

Andrographolide sulfonate (Andro-S), a sulfonation derivative of andrographolide, is a major active ingredient of Xiyanping injection, a traditional Chinese medicine (TCM) commonly used to treat upper respiratory tract infections and pneumonia in China. Andrographolide is a biologically active diterpene isolated from *Andrographis*, an herbaceous plant native to South Asian countries. Sulfonation improves the water solubility and bioavailability of a compound (1). Andro-S exhibits multiple biological functions, including antioxidant, anti-inflammatory, and antineoplastic properties (2-5). Our previous study demonstrated that andrographolide exerts anti-respiratory syncytial virus (RSV) activity by upregulating HO-1 expression in human airway epithelial cells (6).

RSV is a common virus that infects children worldwide. It often causes acute lower respiratory tract infection (ALRI) in young children, which can progress to pneumonia, respiratory failure, and even death. In 2019 alone, there were 2.5–4.1 million RSV infection-associated hospitalizations

in children across 58 countries (7), and about 45% of hospitalizations and in-hospital deaths associated with RSV infection occur in infants younger than six months (8). After pneumococcal pneumonia and *Haemophilus influenzae*, RSV is the third-most common cause of childhood death from ALRI (9). The prophylactic administration of monoclonal antibodies, including palivizumab and nirsevimab, has the potential to mitigate RSV infection among high-risk infants. Nevertheless, this preventive measure offers only transient protection, and its efficacy hinges on the timeliness of intervention in relation to the seasonal RSV surge (10). While the antiviral medication ribavirin can be utilized to treat RSV infection in pediatric patients, the management of severe cases predominantly revolves around supportive measures like oxygen therapy and respiratory support (11,12). Consequently, novel treatment strategies are urgently needed to reduce RSV-associated ALRI and mortality.

Toll-like receptors (TLRs) are key regulators of the immune response to RSV infection (11,13). In particular, TLR3-mediated interferon- $\gamma$  (IFN- $\gamma$ ) response contributes to pulmonary inflammation during RSV infection (14). In this study, we evaluated the effects of Andro-S administered via intranasal and intraperitoneal routes on the pulmonary inflammation caused by RSV infection in immunocompromised mice. The underlying mechanisms associated with TLR3 and IFN- $\gamma$  were also investigated. We present this article in accordance with the ARRIVE reporting checklist (available at <https://jtd.amegroups.com/article/view/10.21037/jtd-24-752/rc>).

## Methods

### Animals

Female BALB/c mice (6–8 weeks old) were purchased from the Laboratory Animal Center at Chongqing Medical University (Chongqing, China) (No. SCXK[Yu] 2012-0001). The mice were maintained in separate cages in a specific-pathogen-free (SPF) facility as described previously (15). To generate immunocompromised

### Highlight box

#### Key findings

- Intranasal administration of andrographolide sulfonate (Andro-S) reduces respiratory syncytial virus (RSV) replication and RSV infection-induced substance inflammation via TLR3-TRIF.

#### What is known and what is new?

- Intraperitoneal injection of Andro-S did not suppress RSV-induced inflammation, whereas intranasal administration reduced the total number of inflammatory cells in the bronchoalveolar lavage fluid (BALF) and pathological damage in the lungs. Furthermore, interferon- $\gamma$  production was significantly decreased in the BALF, as were the N gene and protein expression levels.
- Andro-S aerosol inhalation may be a better treatment for viral respiratory diseases.

#### What is the implication, and what should change now?

- Andro-S may help elucidate the underlying pathology of RSV infection and suggest potential therapeutic targets for the drug development and prevention of RSV-induced diseases.

mice, the animals received a single dose of 100 mg/kg of cyclophosphamide (CYP) via intraperitoneal injection. The mice were randomly assigned to Control group, Andro-S group, RSV group, RSV + Andro-S group with each group consisting of more than four mice. The study protocol was approved by the Ethics Committee of Chongqing Medical University (No. SYXK[Yu] 2012-0001). All animal experiments were in compliance with institutional guidelines for the care and use of animals. A protocol was prepared before the study without registration.

### *RSV production and infection*

The RSV A2 strain was obtained from the Laboratory of Medical Virology at Capital Medical University (Beijing, China). The virus was produced in HEp-2 cells and purified as described previously (16). For RSV infection, the immunocompromised animals received 100  $\mu$ L of intranasal RSV at a total concentration of  $1.0 \times 10^8$  PFU/mL five days after CYP treatment (17). The control group animals received 100  $\mu$ L of PBS.

### *Andro-S treatment*

Mice received intranasal (0.5 mg in 20  $\mu$ L of normal saline) or intraperitoneal (10 mg/kg in 100  $\mu$ L of normal saline) Andro-S (Xiyanping Injection, Jiangxi Qingfeng Pharmaceutical Co. Ltd., Ganzhou, China) two hours after RSV infection (day 0), which was followed by a once-daily administration for four consecutive days (day 1 to day 4). Normal saline served as a negative control. All mice were killed five days after RSV infection. Mice were randomly allocated to different treatment groups, with at least four mice in each treatment group as mentioned earlier.

### *Hematoxylin and eosin (HE) staining*

Pathohistological changes in the lung were evaluated using HE staining. In brief, left lung tissues were fixed in 10% neutral buffered formalin for at least 24 hours. The fixed tissues were dehydrated, embedded in paraffin, and cut into 4-mm sections. The tissue sections were stained with HE and subjected to microscopic analysis. Tissue inflammation was scored as described previously (18).

### *Bronchoalveolar lavage fluid collection*

On day 5, prior to euthanasia, the mice were anesthetized

with intraperitoneal pentobarbital (90 mg/kg). Lungs were lavaged six times. With 0.5 mL of phosphate-buffered saline (PBS) being applied each time. The resulting bronchoalveolar lavage fluid (BALF) was centrifuged at 2,500 rpm for five minutes. The supernatants were stored at  $-80^\circ\text{C}$  for IFN- $\gamma$  analysis. The cell pellets were resuspended in 1 mL of PBS and counted under a microscope to determine total cell counts. To count different types of leukocytes, the cell suspensions were loaded onto microscope slides, air-dried, and stained with Giemsa. A total of 200 cells per sample were counted under a microscope to determine macrophage, lymphocyte, neutrophil, and eosinophil counts.

### *Enzyme-linked immunosorbent assay (ELISA)*

IFN- $\gamma$  levels in the BALF were determined via ELISA (Sizhengbai Biotechnology, Beijing, China) following the manufacturer's directions.

### *Quantitative real-time polymerase chain reaction (qRT-PCR)*

Total RNA was extracted from lung tissues using TRIzol reagent and used for complement DNA (cDNA) synthesis (Takara Bio, Kusatsu, Japan). RSV nucleoprotein (N) messenger RNA (mRNA) levels were determined via qRT-PCR using a hydrolysis probe, as described previously (19,20). The sequences of the hydrolysis probe and primers specific for RSV N are listed in *Table 1*. qRT-PCR was also used to determine the TLR1–9 mRNA levels. The primer sequences specific for TLR1–9 are listed in *Table 2*. Values were normalized to GAPDH expression levels.

### *Western blot analysis*

Total protein was extracted from lung tissues using a protein extraction kit (KeyGEN Biotech Co. Ltd., Nanjing, China). The protein concentrations were determined using a bicinchoninic acid protein assay kit (BioTeke Corporation, Beijing, China). Proteins were separated via gel electrophoresis and transferred onto polyvinylidene difluoride (PVDF) membranes. Western blotting was performed by probing the blocked membranes with primary antibodies specific for RSV N and F (1:1,000; Merck Millipore, Burlington, MA, USA), TLR2 (1:1,000; ABclonal, Woburn, MA, USA), TLR3 (1:1,000; ABclonal), TIR domain-containing adapter-inducing interferon- $\beta$  (TRIF; 1:1,000;

**Table 1** Sequences of the hydrolysis probe and primers specific for RSV N

Name	Primer
Forward primer (5'-3')	AGATCAACTTCTGTCATCCAGCAA
Reverse primer (5'-3')	TTCTGCACATCATAATTAGGAGTATCAAT
Probe	FAM-5'-CACCATCCAACGGAGCACAGGAGAT-3'-BHQ1

RSV N, respiratory syncytial virus nucleoprotein.

**Table 2** Primer sequences specific for TLR1–9

No.	Gene	Forward primer (5'-3')	Reverse primer (5'-3')
1	<i>TLR1</i>	GGTAGCAAGAGAAGTGGTGGAG	CGATGGTGACAGTCAGCAGAAC
2	<i>TLR2</i>	ACAGCAAGGTCTTCCTGGTTCC	GCTCCCTTACAGGCTGAGTTCT
3	<i>TLR3</i>	GTCTTCTGCACGAACCTGACAG	TGGAGGTTCTCCAGTTGGACCC
4	<i>TLR4</i>	AGCTTCTCCAATTTTTCAGAACTTC	TGAGAGGTGGTGTAAGCCATGC
5	<i>TLR5</i>	TCCTGACCAGAGCACATTTGCC	CCTTCAGTGTCCCAAACAGTCG
6	<i>TLR6</i>	TGAGCCAAGACAGAAAACCCA	GGGACATGAGTAAGGTTCTGTG
7	<i>TLR7</i>	ATGTGGACACGGAAGAGACAA	GGTAAGGGTAAGATTGGTGGTG
8	<i>TLR8</i>	AAGTGCTGGACCTGAGCCACAA	CCTCTGTGAGGGTGTAATGCC
9	<i>TLR9</i>	GCTGTCAATGGCTCTCAGTTCC	CCTGCAACTGTGGTAGCTCACT

TLR, Toll-like receptor.

Abcam, Cambridge, UK), and  $\beta$ -actin (1:2,000; Proteintech, Rosemont, IL, USA), respectively. After incubation with the corresponding secondary antibodies, the protein bands were detected using enhanced chemiluminescence (Bio-Rad Laboratories, Hercules, CA, USA).

Statistical analysis

All results are presented as the mean  $\pm$  standard error of the mean (SEM). Data analyses were conducted using SPSS v. 19.0 (IBM Corp., Armonk, NY, USA). One-way analysis of variance (ANOVA) was used to compare the means among three or more groups. The unpaired Student *t*-test was employed to compare the means between two groups. The Pearson method was used for correlation analysis. A *P* value of less than 0.05 was considered statistically significant.

Results

Intranasal but not intraperitoneal Andro-S ameliorated lung inflammation in RSV-infected mice

Healthy BALB/c mice are not susceptible to RSV infection;

however, those whose immune system has been weakened by CYP are vulnerable to RSV infection (21). In this study, BALB/c mice received a single dose of 100 mg/kg of CYP via intraperitoneal injection five days before they were infected intranasally with RSV. In response to RSV infection, the airway epithelium generates chemokines to recruit immune cells to the site of infection to kill virus-infected cells (22). The infiltrating immune cells secrete inflammatory cytokines that cause damage to the lung (23). In this study, RSV infection induced massive infiltration of macrophages, lymphocytes, neutrophils, and eosinophils into the lung, as indicated by the drastically increased counts of these inflammatory cells in the BALF five days after infection (Figure 1A). Similar to our previous findings, elevated IFN- $\gamma$  levels were detected in the BALF of RSV-infected lungs (Figure 1B). HE staining revealed severe bronchiolitis, alveolitis, and perivascular inflammation in the lung five days after RSV infection (Figure 1C), which was reflected in the elevated pathohistological scores of the lungs (Figure 1D). These results were in alignment with previous findings of immunocompromised BALB/c mice developing severe lung inflammation five days after RSV infection. Treatment with intranasal Andro-S

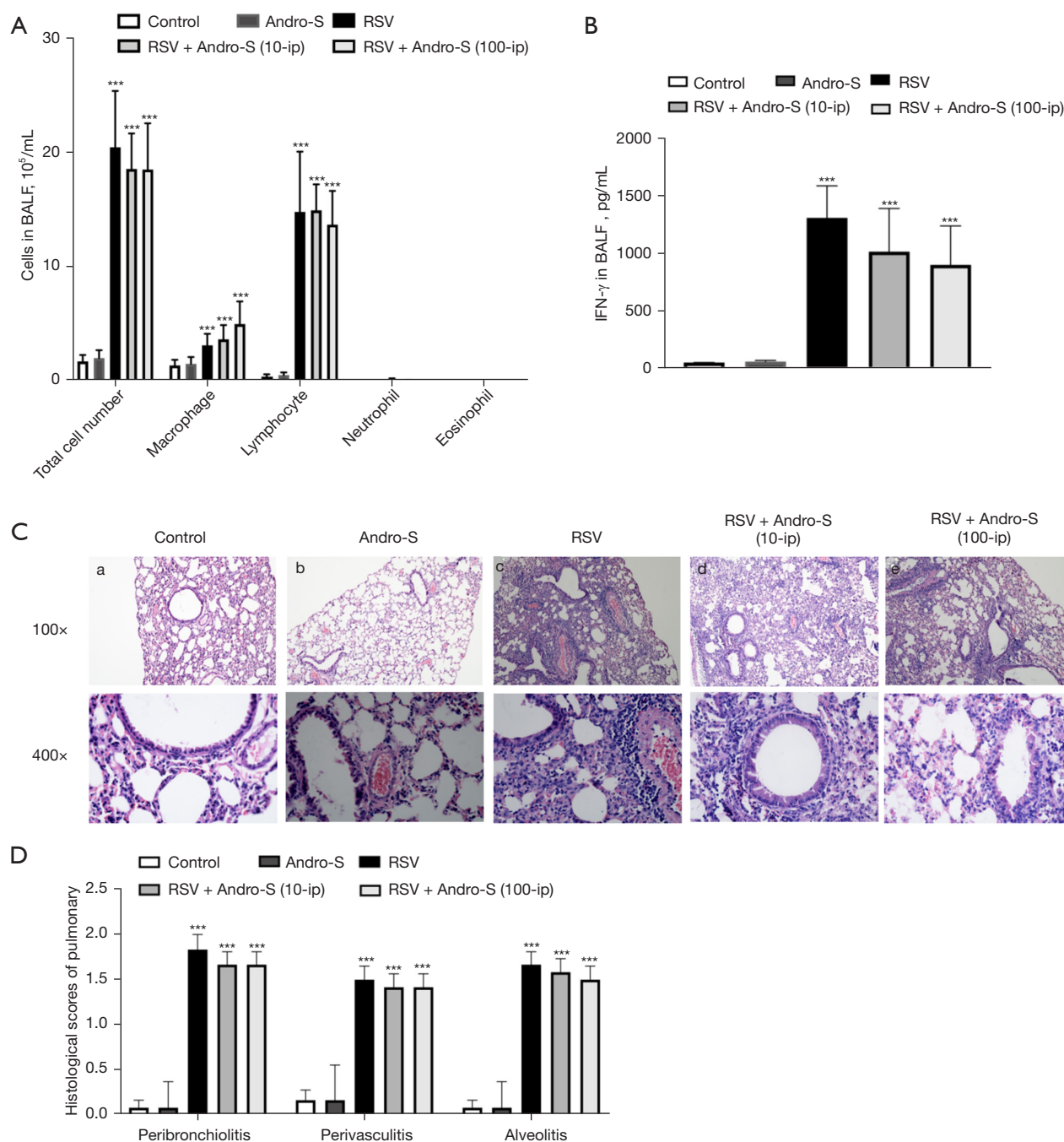


**Figure 1** Effects of intraperitoneal Andro-S on pulmonary inflammation in immunocompromised BALB/c mice five days after RSV infection. (A) Inflammatory cell counts in the BALF. (B) IFN- $\gamma$  levels in the BALF measured via ELISA. (C) Representative images of lung tissues with HE staining showing pathohistological changes in the lung (upper panel: 100 $\times$ ; lower panel: 400 $\times$ ). (a) The control group, (b) the Andro-s group, (c) the RSV group, (d) the RSV mice received intraperitoneal 10 mg/kg of Andro-S, (e) the RSV mice received intraperitoneal 100 mg/kg of Andro-S. (D) Pathohistological scores showing the severity of pulmonary inflammation.  $n \geq 4$ ; \*\*\*,  $P < 0.001$  vs. PBS + saline. RSV, respiratory syncytial virus; Andro-S, andrographolide sulfonate; IFN- $\gamma$ , interferon- $\gamma$ ; BALF, bronchoalveolar lavage fluid; ELISA, enzyme-linked immunosorbent assay; HE, hematoxylin and eosin; PBS, phosphate-buffered saline.



(0.5 mg) postinfection once daily for five consecutive days significantly reduced inflammatory cell infiltration, lowered IFN- $\gamma$  levels, and attenuated inflammation-associated pathohistological changes in the lung (Figure 1A-1D). However, treatment with intraperitoneal Andro-S (10 mg/kg) once daily for five consecutive days demonstrated no significant effects on pulmonary inflammation in infected animals (Figure 2A-2D).

### ***Intranasal Andro-S reduced RSV N and F levels in RSV-infected lungs***

As part of the viral ribonucleoprotein complex, RSV N is essential for viral RNA replication, mRNA transcription, and virus assembly and encapsulation (24). Therefore, RSV N is commonly used as a marker of viral load during RSV infection. In this study, RSV N mRNA and protein levels in the lung were detected via qRT-PCR and Western blot analysis, respectively. As shown in Figure 3A,3B, RSV N was detected in infected but not in uninfected lungs. We also detected a positive correlation between total inflammatory cell count and RSV N mRNA ( $P=0.01$ ;  $r=0.99$ ) and between IFN- $\gamma$  and RSV N mRNA ( $P=0.01$ ;  $r=0.99$ ). These results indicated that higher viral load induced more intense immune response. Intranasal Andro-S significantly reduced RSV N mRNA and protein levels in infected lungs (Figure 3A,3B), suggesting that Andro-S protected against RSV infection at least partially by inhibiting viral RNA replication and encapsulation, thereby reducing viral load. The RSV fusion protein (F) mediates the fusion of viral and host cell membranes to facilitate virus entry (24). In this study, Andro-S also reduced RSV F protein levels in infected lungs (Figure 3B), suggesting that Andro-S also could have reduced viral load by blocking virus entry.

### ***Intranasal Andro-S downregulated TLR3 and TRIF in RSV-infected lungs***

To investigate the role of TLRs as possible mediators of Andro-S, we evaluated the mRNA expression of TLR1–9 in lung tissues using qRT-PCR (Figure 4). We found that RSV infection induced *TLR1*, *TLR2*, *TLR3*, and *TLR9* mRNA expression (Figure 4A-4C,4I) but downregulated *TLR5* expression (Figure 4E). Intranasal Andro-S reduced *TLR2* and *TLR3* mRNA expression in RSV-infected lungs (Figure 4B,4C), but showed no significant effects on *TLR1*, *TLR5*, or *TLR9* (Figure 4A,4E,4I). Neither RSV infection

nor Andro-S significantly changed the mRNA expression of *TLR4*, *TLR6*, *TLR7*, or *TLR8* (Figure 4D,4F-4H). Next, we evaluated the protein expression of *TLR2*, *TLR3*, and *TRIF*, a critical adaptor for *TLR3*, in lung tissues using Western blot analysis. We found that RSV infection did not cause significant changes in *TLR2* protein expression but did increase the protein expression of *TLR3* and *TRIF* in the lung (Figure 5A-5E). Intranasal Andro-S demonstrated no effects on *TLR2* protein expression but did downregulate both *TLR3* and *TRIF* protein expression in RSV-infected lungs (Figure 5A-5E). These findings suggested that intranasal Andro-S ameliorated inflammation in RSV-infected lungs by downregulating *TLR3* and *TRIF* protein expression in the lung.

## **Discussion**

RSV infection in infants remains a global public health concern, necessitating the development of novel therapies. In this study, we found that intranasal administration of Andro-S ameliorated RSV infection-associated lung inflammation in immunocompromised BALB/c mice. In terms of mechanism, intranasal Andro-S reduced viral load and downregulated *TLR3* and its adaptor *TRIF* in infected lungs.

RSV infection triggers an initial innate immune response, primarily involving airway epithelial cells and tissue-resident dendritic cells and macrophages. These cells activate the recruitment of lymphocytes and granulocytes to the site of infection, which then begin to eliminate the virus and mediate further recruitment of adaptive immune cells (25). These innate and adaptive immune responses cause airway inflammation and damage. In this study, we detected severe bronchiolitis, alveolitis, and pulmonary perivascular inflammation accompanied by inflammatory cell infiltration five days after RSV infection. Daily intranasal Andro-S administration for five consecutive days, starting two hours after the infection, effectively reduced inflammatory cell infiltration and attenuated inflammation-associated pathohistological changes in the lung. Given that early intervention and viral clearance are important factors in determining the prognosis of viral infections, the findings from this study demonstrate that intranasal administration of Andro-S may hold promise as an effective early intervention after RSV infection in controlling airway inflammation and improving patient outcomes.

Compared with other drug delivery routes, intranasal

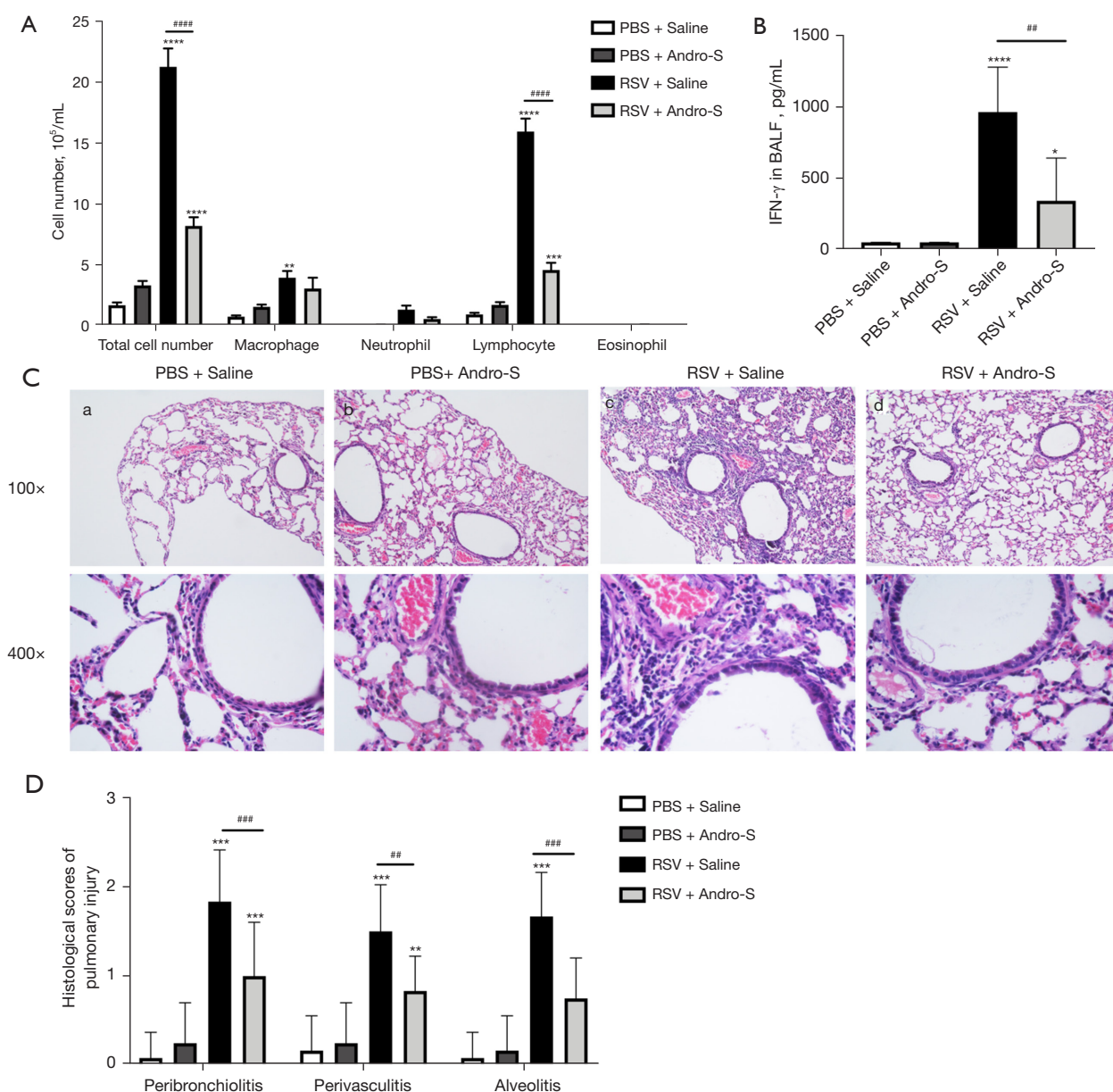


**Figure 2** Effects of intranasal Andro-S on pulmonary inflammation in immunocompromised BALB/c mice five days after RSV infection. (A) Inflammatory cell counts in the BALF. (B) IFN- $\gamma$  levels in the BALF measured via ELISA. (C) Representative images of lung tissues with HE staining showing pathohistological changes in the lung (upper panel: 100 $\times$ ; lower panel: 400 $\times$ ). (a) the PBS + saline group, (b) the PBS + Andro-S group, (c) the RSV + saline group, (d) the RSV mice received intranasal Andro-S. (D) Pathohistological scores showing the severity of pulmonary inflammation.  $n \geq 4$ . \*,  $P < 0.05$ ; \*\*,  $P < 0.01$ ; \*\*\*,  $P < 0.001$ , \*\*\*\*,  $P < 0.0001$  vs. PBS + saline; #,  $P < 0.01$ ; ##,  $P < 0.001$ ; ###,  $P < 0.0001$ . RSV, respiratory syncytial virus; Andro-S, andrographolide sulfonate; IFN- $\gamma$ , interferon- $\gamma$ ; BALF, bronchoalveolar lavage fluid; ELISA, enzyme-linked immunosorbent assay; HE, hematoxylin and eosin; PBS, phosphate-buffered saline.

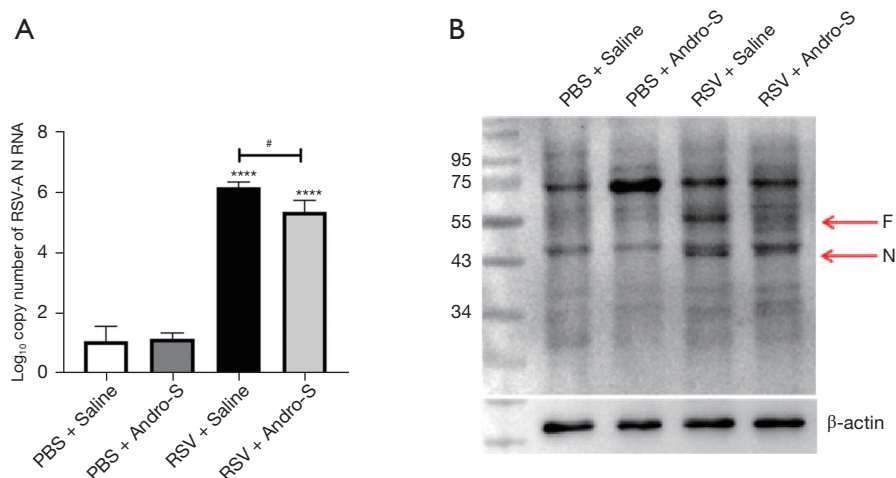


**Figure 3** Effects of intranasal Andro-S on RSV N and F expression in the lungs of immunocompromised BALB/c mice five days after RSV infection. (A) Relative copy number of RSV-A N mRNA as determined via qRT-PCR.  $n \geq 4$ . \*\*\*\*,  $P < 0.0001$  vs. PBS + saline; #,  $P < 0.05$ . (B) Representative Western blotting gel images showing RSV N and F protein expression. RSV, respiratory syncytial virus; PBS, phosphate-buffered saline; Andro-S, andrographolide sulfonate; qRT-PCR, quantitative real-time polymerase chain reaction.

administration directly delivers the drug to the airway with reduced systemic exposure. Thus, it is a preferred method for the administration of lung-targeting drugs such as those for the treatment of respiratory diseases. For example, intranasal administration of a long-acting ACE2 protein showed superior performance over intraperitoneal injection of the same therapeutic protein in the k18-hACE2 mouse model of severe acute respiratory syndrome-related coronavirus 2 (SARS-CoV-2) infection (26). In this study, RSV infection-induced lung inflammation was reduced by intranasal but not intraperitoneal administration of Andro-S, indicating that intranasal administration is a suitable drug delivery method for the treatment of RSV infection and associated airway conditions. In recent years, a growing number of TCMs have been reformulated as aerosol (spray) drugs and have shown clinical efficacy and safety (27). For example, oral inhalation of the TCM Kaihoujian aerosol significantly reduced acute laryngitis in adults and alleviated vocal cord leukoplakia (28). Similarly, Andro-S may be reformulated in the future for inhalation in the treatment of RSV infection.

In this study, intranasal Andro-S reduced the protein levels of RSV N and F in infected lungs, suggesting that it reduced viral load by inhibiting virus entry and replication. The mechanisms by which Andro-S downregulates these

viral proteins are not clear and require further investigation. Functioning as pattern recognition receptors (PRRs) for RSV-derived pathogen-associated molecular patterns (PAMPs), TLRs play an important role in initiating immune response to RSV infection (11). In particular, TLR3-mediated IFN- $\gamma$  response has been shown to contribute to pulmonary inflammation during RSV infection (17,28). Of note, TLR3-mediated type II IFN response is considered to be a critical contributor to antiviral innate immunity (29). In this study, RSV-infected lungs exhibited increased protein expression of TLR3 and its adaptor TRIF, as well as elevated IFN- $\gamma$  levels in the BALF, which is in line with our previous research (17). A study has shown that andrographolide can inhibit TRIF-dependent TLR signaling by targeting TANK binding kinase 1 (TBK1) (30). In this study, intranasal Andro-S downregulated TLR3 and TRIF in infected lungs and reduced IFN- $\gamma$  levels in the BALF, suggesting that Andro-S ameliorated lung inflammation caused by RSV infection by downregulating the TLR3-TRIF-IFN- $\gamma$  axis. Previous studies have also reported that Andro-S can protect against inflammatory cell injury by antagonizing nuclear factor- $\kappa$ B (NF- $\kappa$ B) and activating Nrf2 antioxidant response (31,32). In addition, Andro-S was found to alleviate poly (I:C)-induced pneumonia in mice by downregulating NF- $\kappa$ B (33). Hypothetically,



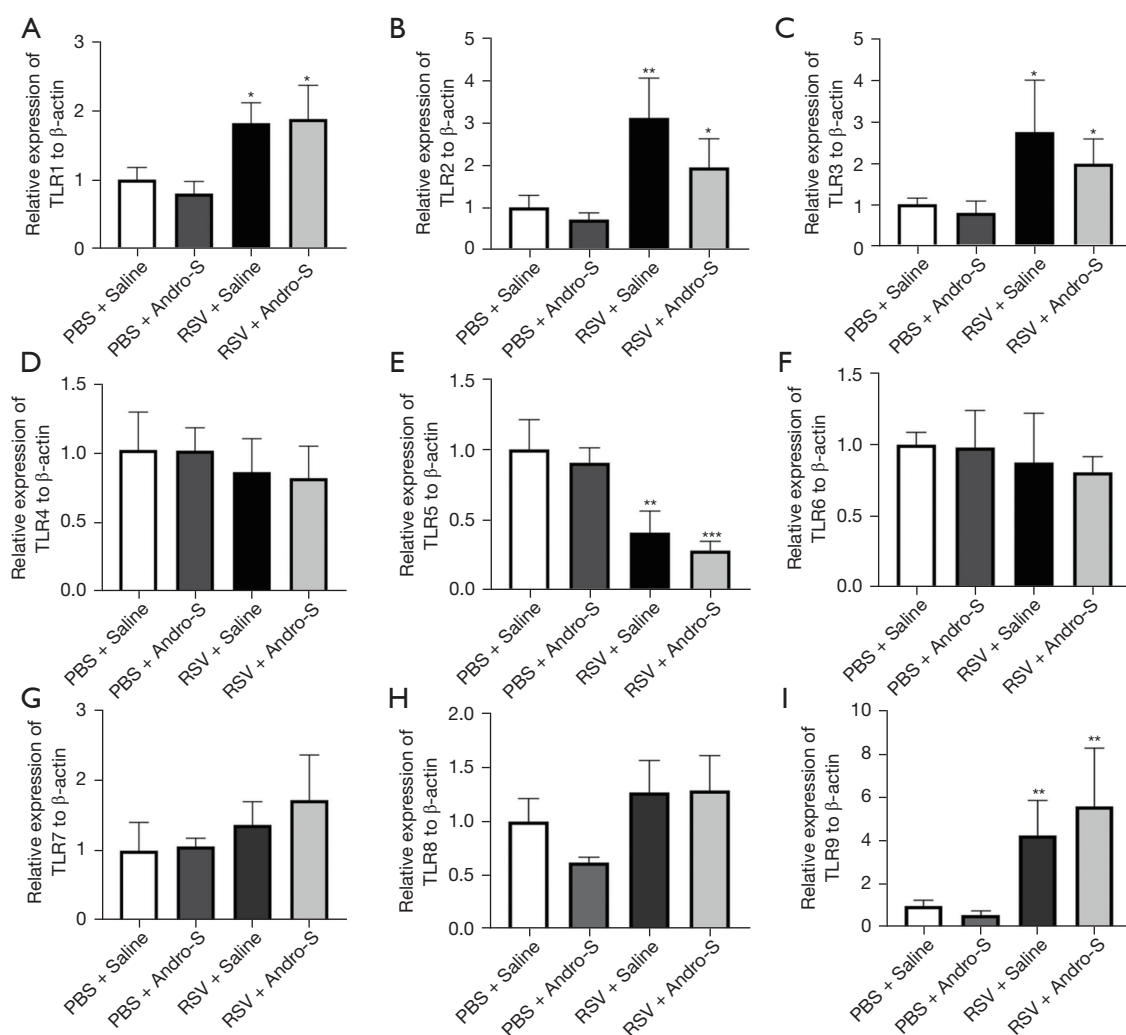


**Figure 4** Effects of intranasal Andro-S on TLR1–9 mRNA expression in the lungs of immunocompromised BALB/c mice five days after RSV infection. Relative mRNA levels of TLR1 (A), TLR2 (B), TLR3 (C), TLR4 (D), TLR5 (E), TLR6 (F), TLR7 (G), TLR8 (H), and TLR9 (I) in lung tissues as determined by qRT-PCR.  $n \geq 4$ . \*,  $P < 0.05$ ; \*\*,  $P < 0.01$ ; \*\*\*,  $P < 0.001$  vs. PBS + saline. TLR, Toll-like receptor; RSV, respiratory syncytial virus; PBS, phosphate-buffered saline; Andro-S, andrographolide sulfonate; qRT-PCR, quantitative real-time polymerase chain reaction.

these anti-NF- $\kappa$ B and antioxidant properties of Andro-S may also mediate its protective effects against airway inflammation caused by RSV infection. Future *in vitro* and/or *in vivo* experiments are required to investigate this hypothesis.

## Conclusions

Intranasal but not intraperitoneal administration of Andro-S ameliorated the lung inflammation caused by RSV infection in mice by suppressing the TLR3-TRIF-IFN- $\gamma$  axis. Andro-S inhalation aerosol may be used to treat RSV

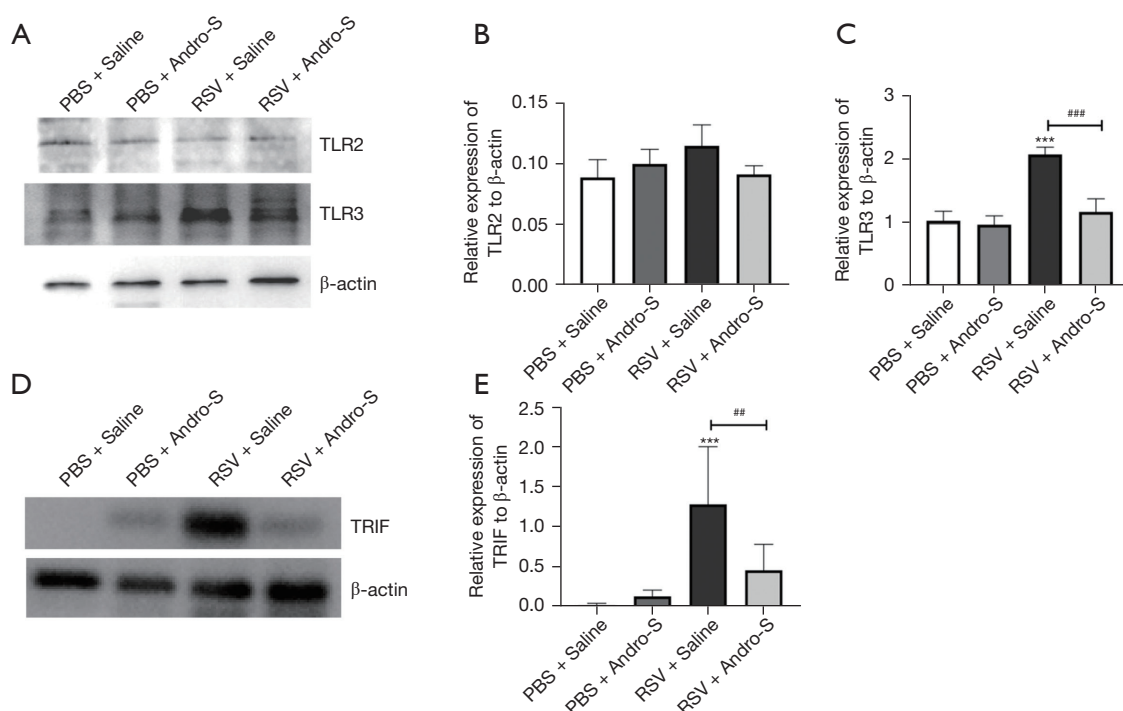


**Figure 5** Effects of intranasal Andro-S on TLR2, TLR3, and TRIF protein expression in the lungs of immunocompromised BALB/c mice five days after RSV infection. (A) Representative Western blotting gel images showing TLR2 and TLR3 protein expression in the lung. (B,C) Relative protein levels of TLR2 (B) and TLR3 (C) in the lung. (D) Representative Western blotting gel images showing TRIF protein expression in the lung. (E) Relative protein levels of TRIF in the lung.  $n \geq 4$ . \*\*\*,  $P < 0.001$  vs. PBS + saline; #,  $P < 0.01$ ; ###,  $P < 0.001$ . RSV, respiratory syncytial virus; PBS, phosphate-buffered saline; Andro-S, andrographolide sulfonate; TRIF, TIR domain-containing adapter-inducing interferon- $\beta$ .

infection-associated airway conditions and reduce mortality.

## Acknowledgments

**Funding:** This work was funded by the Chongqing Natural Science Foundation Project (No. CSTB2022NSCQ-MSX0129) and the Open Project of the State Key Laboratory of Innovative Natural Medicine and TCM Injections (No. QFSKL2020020).

## Footnote

**Reporting Checklist:** The authors have completed the ARRIVE reporting checklist. Available at <https://jtd.amegroups.com/article/view/10.21037/jtd-24-752/rc>

**Data Sharing Statement:** Available at <https://jtd.amegroups.com/article/view/10.21037/jtd-24-752/dss>

**Peer Review File:** Available at <https://jtd.amegroups.com/article/view/10.21037/jtd-24-752/prf>

**Conflicts of Interest:** All authors have completed the ICMJE uniform disclosure form (available at <https://jtd.amegroups.com/article/view/10.21037/jtd-24-752/coif>). Y.L. is employed by Jiangxi Qingfeng Pharmaceutical Co., Ltd. (Jiangxi, China). The other authors have no conflicts of interest to declare.

**Ethical Statement:** The authors are accountable for all aspects of the work in ensuring that questions related to the accuracy or integrity of any part of the work are appropriately investigated and resolved. The study protocol was approved by the Ethics Committee of Chongqing Medical University (No. SYXK[Yu] 2012-0001). All animal experiments were in compliance with institutional guidelines for the care and use of animals.

**Open Access Statement:** This is an Open Access article distributed in accordance with the Creative Commons Attribution-NonCommercial-NoDerivs 4.0 International License (CC BY-NC-ND 4.0), which permits the non-commercial replication and distribution of the article with the strict proviso that no changes or edits are made and the original work is properly cited (including links to both the formal publication through the relevant DOI and the license). See: <https://creativecommons.org/licenses/by-nc-nd/4.0/>.

## References

1. Zheng D, Shao J, Chen W, et al. In vitro Metabolism of Sodium 9-dehydro-17-hydro-andrographolide-19-yl Sulfate in Rat Liver S9 by Liquid Chromatography-Mass Spectrometry Method. *Pharmacogn Mag* 2016;12:S102-8.
2. Burgos RA, Alarcón P, Quiroga J, et al. Andrographolide, an Anti-Inflammatory Multitarget Drug: All Roads Lead to Cellular Metabolism. *Molecules* 2020;26:5.
3. Lin FL, Wu SJ, Lee SC, et al. Antioxidant, antioedema and analgesic activities of *Andrographis paniculata* extracts and their active constituent andrographolide. *Phytother Res* 2009;23:958-64.
4. Mussard E, Jousselin S, Cesaro A, et al. *Andrographis paniculata* and Its Bioactive Diterpenoids Protect Dermal Fibroblasts Against Inflammation and Oxidative Stress. *Antioxidants (Basel)* 2020;9:432.
5. Kumar RA, Sridevi K, Kumar NV, et al. Anticancer and immunostimulatory compounds from *Andrographis paniculata*. *J Ethnopharmacol* 2004;92:291-5.
6. Che S, Zhou N, Liu Y, et al. Andrographolide exerts anti-respiratory syncytial virus activity by up-regulating heme oxygenase-1 independent of interferon responses in human airway epithelial cells. *Mol Biol Rep* 2023;50:4261-72.
7. Li Y, Johnson EK, Shi T, et al. National burden estimates of hospitalisations for acute lower respiratory infections due to respiratory syncytial virus in young children in 2019 among 58 countries: a modelling study. *Lancet Respir Med* 2021;9:175-85.
8. Shi T, McAllister DA, O'Brien KL, et al. Global, regional, and national disease burden estimates of acute lower respiratory infections due to respiratory syncytial virus in young children in 2015: a systematic review and modelling study. *Lancet* 2017;390:946-58.
9. Nair H, Nokes DJ, Gessner BD, et al. Global burden of acute lower respiratory infections due to respiratory syncytial virus in young children: a systematic review and meta-analysis. *Lancet* 2010;375:1545-55.
10. Li Y, Hodgson D, Wang X, et al. Respiratory syncytial virus seasonality and prevention strategy planning for passive immunisation of infants in low-income and middle-income countries: a modelling study. *Lancet Infect Dis* 2021;21:1303-12.
11. Klein Klouwenberg P, Tan L, Werkman W, et al. The role of Toll-like receptors in regulating the immune response against respiratory syncytial virus. *Crit Rev Immunol* 2009;29:531-50.
12. Malik S, Ahmad T, Muhammad K, et al. Respiratory Syncytial Virus Infection: Treatments and Clinical Management. *Vaccines (Basel)* 2023;11:491.
13. Moin AT, Ullah MA, Patil RB, et al. A computational approach to design a polyvalent vaccine against human respiratory syncytial virus. *Sci Rep* 2023;13:9702.
14. Boukhvalova MS, Sotomayor TB, Point RC, et al. Activation of interferon response through toll-like receptor 3 impacts viral pathogenesis and pulmonary toll-like receptor expression during respiratory syncytial virus and influenza infections in the cotton rat *Sigmodon hispidus* model. *J Interferon Cytokine Res* 2010;30:229-42.
15. Xie J, Long X, Gao L, et al. Respiratory Syncytial Virus Nonstructural Protein 1 Blocks Glucocorticoid Receptor Nuclear Translocation by Targeting IPO13 and May Account for Glucocorticoid Insensitivity. *J Infect Dis* 2017;217:35-46.
16. Zang N, Li S, Li W, et al. Resveratrol suppresses persistent airway inflammation and hyperresponsiveness might partially via nerve growth factor in respiratory syncytial virus-infected mice. *Int Immunopharmacol* 2015;28:121-8.
17. Zang N, Xie X, Deng Y, et al. Resveratrol-mediated gamma interferon reduction prevents airway inflammation and airway hyperresponsiveness in respiratory syncytial virus-infected immunocompromised mice. *J Virol* 2011;85:13061-8.
18. Peebles RS Jr, Sheller JR, Collins RD, et al. Respiratory syncytial virus infection does not increase allergen-induced type 2 cytokine production, yet increases airway hyperresponsiveness in mice. *J Med Virol* 2001;63:178-88.
19. Zhou N, Li W, Ren L, et al. An Interaction of LPS and RSV Infection in Augmenting the AHR and Airway Inflammation in Mice. *Inflammation* 2017;40:1643-53.
20. Chen S, Yu G, Xie J, et al. High-mobility group box-1 protein from CC10+ club cells promotes type 2 response in the later stage of respiratory syncytial virus infection. *Am J Physiol Lung Cell Mol Physiol* 2019;316:L280-L290.
21. Kong X, Hellermann GR, Patton G, et al. An immunocompromised BALB/c mouse model for

- respiratory syncytial virus infection. *Viol J* 2005;2:3.
22. Guo-Parke H, Canning P, Douglas I, et al. Relative respiratory syncytial virus cytopathogenesis in upper and lower respiratory tract epithelium. *Am J Respir Crit Care Med* 2013;188:842-51.
  23. Moreno-Solís G, Torres-Borrego J, de la Torre-Aguilar MJ, et al. Analysis of the local and systemic inflammatory response in hospitalized infants with respiratory syncytial virus bronchiolitis. *Allergol Immunopathol (Madr)* 2015;43:264-71.
  24. Collins PL, Fearn R, Graham BS. Respiratory syncytial virus: virology, reverse genetics, and pathogenesis of disease. *Curr Top Microbiol Immunol* 2013;372:3-38.
  25. Griffiths C, Drews SJ, Marchant DJ. Respiratory Syncytial Virus: Infection, Detection, and New Options for Prevention and Treatment. *Clin Microbiol Rev* 2017;30:277-319.
  26. Hassler L, Wysocki J, Ahrendsen JT, et al. Intranasal soluble ACE2 improves survival and prevents brain SARS-CoV-2 infection. *Life Sci Alliance* 2023;6:e202301969.
  27. Xie W, Zhang Y, Tang J, et al. Efficacy and Safety of Traditional Chinese Medicines as a Complementary Therapy Combined With Chemotherapy in the Treatment of Gastric Cancer: An Overview of Systematic Reviews and Meta-Analyses. *Integr Cancer Ther* 2024;23:15347354231225961.
  28. Feng W, Chen H, Lu Y, et al. Comparing the efficacy and safety of atomization of traditional Chinese medicine Kai Hou Jian and budesonide suspension in adult acute laryngitis: a randomized control trial. *Ann Transl Med* 2022;10:1019.
  29. Negishi H, Osawa T, Ogami K, et al. A critical link between Toll-like receptor 3 and type II interferon signaling pathways in antiviral innate immunity. *Proc Natl Acad Sci U S A* 2008;105:20446-51.
  30. Kim AY, Shim HJ, Shin HM, et al. Andrographolide suppresses TRIF-dependent signaling of toll-like receptors by targeting TBK1. *Int Immunopharmacol* 2018;57:172-80.
  31. Xu Y, Tang D, Wang J, et al. Neuroprotection of Andrographolide Against Microglia-Mediated Inflammatory Injury and Oxidative Damage in PC12 Neurons. *Neurochem Res* 2019;44:2619-30.
  32. Fu K, Chen H, Wang Z, et al. Andrographolide attenuates inflammatory response induced by LPS via activating Nrf2 signaling pathway in bovine endometrial epithelial cells. *Res Vet Sci* 2021;134:36-41.
  33. Cui J, Gao J, Li Y, et al. Andrographolide sulfate inhibited NF-κB activation and alleviated pneumonia induced by poly I:C in mice. *J Pharmacol Sci* 2020;144:189-96.

**Cite this article as:** Zhou N, Che S, Liu J, Jiang Z, Ren L, Liu Y, Liu E, Xie J. Andrographolide sulfonate downregulation of TLR3-TRIF and amelioration of airway inflammation caused by respiratory syncytial virus infection. *J Thorac Dis* 2024;16(7):4607-4618. doi: 10.21037/jtd-24-752